Efficient 3D Semantic Segmentation of Seismic Images using Orthogonal Planes 2D Convolutional Neural Networks

Arthur Bridi Guazzelli
Statistics and Computer Science Dept.
Federal University of Santa Catarina
Florianópolis, Brazil
arthur.bg@grad.ufsc.br

Mauro Roisenberg
Statistics and Computer Science Dept.
Federal University of Santa Catarina
Florianópolis, Brazil
mauro.roisenberg@ufsc.br

Bruno B. Rodrigues
Petrobras S.A.
CENPES Research Center
Rio de Janeiro, Brazil
bbrodrigues@petrobras.com.br

***Abstract*—Technological advances in oil and gas reservoir characterization such as 3D seismics and seismic attributes enriched the subsurface's description made by specialists. Nevertheless, the analysis of this now huge volume of data became a complex task. This work explores the use of 2D orthogonal planes convolutional neural networks for 3D seismic cube facies classification, one of the steps of reservoir characterization. Through a sampling method that captures spatial information of seismic data, the proposed model were applied in both synthetic data of the Stanford VI-E reservoir and in a benchmark based on the F3 block, which is part of a real reservoir. Compared to other models in the same benchmark, the classifiers produced here had superior results, with over 88% in pixel accuracy and 90% class accuracy on some instances. The sampling method is also flexible to use in practical cases.**

***Index Terms*—Convolutional Neural Network, Orthogonal Planes Model, 3D Segmentation, Seismic Image Processing, Reservoir Characterization.**

I. Introduction

The process of reservoir characterization is one of the most important tasks during the study of an oil field. Using data from different sources, scales and methods, such as seismic data, well logs, production data, rock physics analysis, etc. many models of the subsurface can be generated to give a better understanding of the area under study. From an economic point of view, an accurate reservoir description provides better expected return and is a cornerstone for crucial decision making, such as potential new well locations [1].

One of the steps in this process is the classification of seismic facies. A seismic facies is a three dimensional sedimentary unit composed by groups of reflection patterns that differ from those of other adjacent facies and are generally related to depositional or geological structures, or even with fluid type changes [2]. This task is performed by specialists analyzing sections of the seismic data or derived seismic attributes. As the amount of available data increased and different seismic attributes appeared, this task grew in complexity and became intractable for humans to perform. Unsupervised machine learning algorithms and statistical methods e.g. self-organizing maps and PCA became popular tools for the geoscientist to deal with this large amount of data. Nevertheless, such methods still required feature extraction to be performed manually.

Automated detection and classification of geological structure elements, such as salt domes, channels, faults and folds, from seismic images provides an important first step towards new generation of geological interpretation tools [3].

Deep learning algorithms have been proposed as an alternative to solve the problems presented by manual classification of seismic facies. Recent research shows that Convolutional neural networks (CNNs) is one of the most promising techniques to apply to amplitude data for seismic data classification. According to [4], the main advantages of CNN over other supervised classification methods are it's spatial awareness and automatic feature extraction. For image classification problems, other than using the intensity values at each pixel individually, CNN analyzes the patterns among pixels in an image, like textures, edges, etc. [4] [5] [6].

While the facies classification is usually done trace-by-trace, or more commonly on a 2D inline or crossline seismic image, significant challenges still exist for seismic facies classification in a 3D seismic volume [7].

As seismic facies are essentially three dimensional geobodies, we believe that volumetric or spatial context processing tools are a natural way of achieving better results in automatic seismic classification. In this sense, 3D CNNs could be used to improve the identification of 3D volumes, such as tomography and seismic images. However, 3D CNNs is still at an early stage due to their complexity. With the goal of maintaining simplicity while incorporating 3-dimensional image processing capability, this paper proposes the use of Three Orthogonal Planes convolutional neural network model (TOP-CNN), a model partially inspired by the LBP-TOP and T-CNN models proposed by [8] and [9] respectively and the work of [10].

This work uses a patch-based model in which we extract 3 orthogonal cross-sections planes from a 3D sample of the

This work was partially supported under grant no. 5850.0105377.17.9 by Petrobras S.A.

978-1-7281-6926-2/20/$31.00 ©2020 IEEE

seismic cube in order to create a 2D image as input — much like a RGB image. For training examples, the label for the whole image is derived from the center where the 3 planes intersect each other. Applying our model on data from both Stanford VI-E synthetic model and on a benchmark [11] based on the F3 block, we concluded that our model achieved better results when compared with 2D CNN trained with the same data arranged as sequential slices, without the computational complexity of using 3D CNN.

II. Related Work

In the petroleum exploration industry, seismic data is one of the fundamental sources used to interpret subsurface geology [12]. Classifying and interpreting the depositional patterns that form the various subsurface structures can provide valuable clues as to whether the area of interest can contain hydrocarbons in a viable way and whether further research is warranted.

A Seismic Facies is a three dimensional seismic unit composed of groups of reflections whose parameters differ from those of adjacent facies units [13] [2].

Seismic facies classification refers to the interpretation of facies type from the seismic reflector information [4]. In addition, the classification of seismic facies can provide important insights about the various depositional units, such as: grain size, mineralogy, porosity and permeability.

Automatic classification of seismic facies using machine learning techniques has been of great interest to researchers in the last 15 years. The first researches were directed to the application of supervised and unsupervised methods. Coléou et al. [14] provides an embracing review on unsupervised methods. Zhao et al. [15] reviewed and compared six supervised and unsupervised methods applying them to a 3D seismic data volume from a turbidite system. They analyzed the importance of the choice of the correct input attributes.

In recent years, there has been great interest in using fully-supervised deep learning and CNN models for seismic facies classification. The main advantages of CNN over other supervised classification methods are its spatial awareness and automatic feature extraction [11]. [4], [5], [16] and others showed application of state-of-the-art image classification and deep learning algorithms in stacked 2D sections of seismic data .

From the image processing point of view, seismic facies classification brings a series of challenges: it can be considered indeed a segmentation problem as it aims to distinguish and segment different geological structures within the same image; training data availability is much sparser comparing to classical image classification problems, there is a lack of large publicly-available annotated datasets for seismic interpretation; the annotation process is time-consuming, requires subject matter expertise, and can be quite subjective; data is always contaminated by noise and the separation between different rock bodies are rarely explicitly defined [4] [11].

Zhao [4] describes and compares 2 CNNs models for seismic facies classification: the patch-based model, in which the output from the network is a single value representing the facies label of the seismic sample at the center of the input patch; and the encoder-decoder fully convoltional neural network (FCN) model, which classifies all samples in a seismic line simultaneously. According to him, the encoder-decoder model provides superior seismic facies classification quality comparing to the traditional patch-based CNN.

Chevitarese et al. [5] presented deep learning models specifically for the task of classification of seismic facies along with a detailed discussion on how different parameters may affect the model's performance. They proposed many variations of a fully convolutional neural network model (Danet-FCN) that can distinguish different seismic facies with resolution equal to the pixel size.

Alaudah et al. [11] provided a benchmark for comparing the results of different machine learning approaches for facies classification. They made available a fully annotated 3D geological dataset of the Netherlands F3 Block along with two baseline models that differ in the way they are trained and the way they are used to label the seismic volume. Their so-called patch-based model is trained on small patches extracted from the inlines and crosslines of the training data. The section-based model is trained on entire inline and crossline sections. This models were analyzed for facies classification based on the encoder-decoder FCN architecture they called deconvolution network. They also proposed many evaluation metrics as a scheme for evaluating other models on these datasets.

In all these works, facies segmentation maps are predicted for a full volume by taking predictions one slice at a time. This means that they inherently fail to leverage context from adjacent slices. Voxel information from adjacent slices may be useful for the prediction of segmentation map [17].

Few studies use 3D convolution in the segmentation of seismic images. Jiang [18] segments geophysical structures such as channels and faults in 3D seismic volumes. He applies CNN as a local classifier to 2D and 3D patches around every voxel in the seismic volume in order to perform semantic segmentation. In his experiments, 3D CNN showed big improvement compared to 2D CNN. Wu et al [19] perform an efficient image-to-image fault segmentation by using a supervised 3D convolutional neural network. They claim that the 3D CNN can predict faults from 3D seismic images much more accurately and efficiently than conventional methods.

Despite the similarity between seismic image segmentation and biomedical image segmentation, 3D convolutional networks have been more frequently applied in this last type of application [20] [21] [22].

Three Orthogonal Planes networks appear in some research as simpler alternatives to 3D fully convolutional networks in other types of applications. Andrearczyk and Whelan [9] developed a new approach to Dynamic Texture (DT) analysis based on a CNN method applied on three orthogonal planes xy, xt and yt . They trained CNNs on spatial frames and temporal slices extracted from the DT sequences and combined their outputs to obtain a competitive DT classifier. Their model is inspired by the seminal work of Zhao and Pietikäinen [8] in

which a volume Local Binary Patterns (LBP) method was developed to combine the motion and appearance together. A simpler LBP-TOP operator based on concatenated LBP histograms computed from three orthogonal planes was also presented, making it easy to extract co-occurrence features from a larger number of neighboring points. Pourtaherian et al. [10] applied orthogonal-plane convolutional neural networks for semantic needle detection in a 3D ultrasound volume. The method was able to accurately detect even very short needles, ensuring that the needle and its tip are maximally visible in the visualized plane during the entire intervention.

III. Proposed Method

In this work we developed a deep neural network architecture whose idea is simple, but which offers a robust and efficient alternative to semantic segmentation of objects in 3D volumes, such as in tomography images and seismic cubes. In this class of applications, the joint analysis of the object's three-dimensional shape is very important for the segmentation task and its analysis represents a gain compared to techniques that seek to do the segmentation based only on multi-slices of two-dimensional images. On the other hand, the use of 3D convolution operations would represent a high computational complexity for training and applying the model.

In the present study we used a patch-based CNN model called Three Orthogonal Planes convolutional neural network model(TOP-CNN). According to [4], semantic segmentation in tomographic images can be done with patch-based or using encoder-decoder CNN models. A basic patch-based model consists of several convolutional layers, pooling (downsampling) layers, and fully-connected layers. The output from the network is a single value representing the facies (class) label of the seismic sample at the center of the input patch.

The central idea of our method is to use classic and well-known models of CNN networks, such as AlexNet or VGG, using state-of-the-art concepts and tools to train, in which the receptive fields of the RGB channels of the network input layer are re-organized in orthogonal planes in order to receive as inputs signals a set of 2D images from 3 orthogonal planes of the sub-volume to be segmented, as can be seen in Figure 1.

For an input image (for seismic data: amplitudes in orthogonal planes crossing the central a point of a small 3D window), the TOP-CNN model first automatically extracts several high-level abstractions of the three 2D images (similar to seismic attributes) using the convolutional and pooling layers, then classifies the extracted attributes using the fully connected and softmax layers.

For each example used as a network input, a subsampling of the seismic cube to a cube of dimensions $n \times n \times n$ is made. The classification objective is the central point of this sample, that is, we want to identify which facies this central point belongs to. The size chosen for sampling imposes a spatial restriction on the network, since learning is carried out based on individual examples. As the model uses 2D convolution, it is necessary to transform the information of the sampled cube

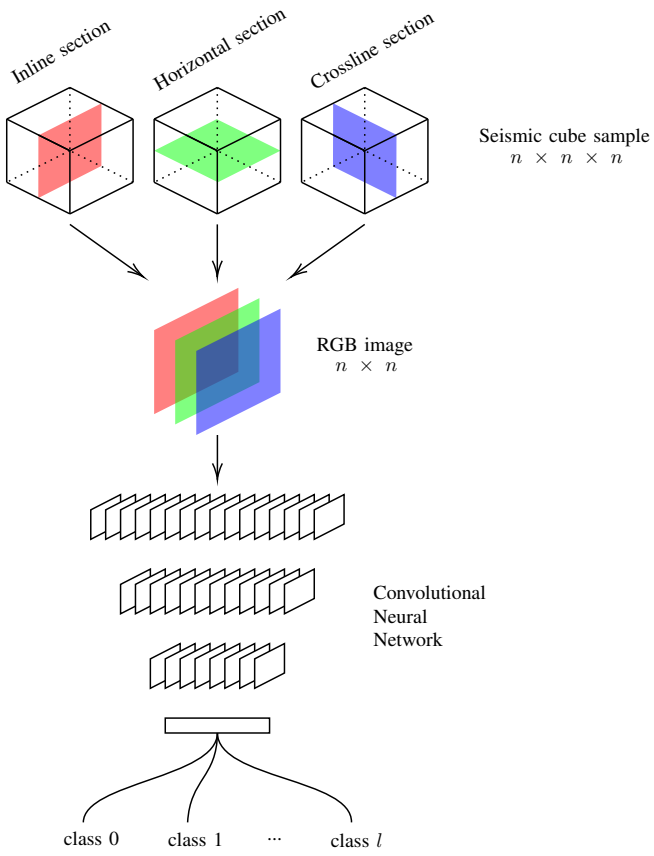

Fig. 1: Overview of our proposed method using 3 orthogonal planes sampling to create inputs for a convolutional neural network.

so that it adapts to the two-dimensional format that feeds the model. The objective is to carry out this transformation without losing the spatial correlations in the three dimensions of the cube and, for this, three sections are extracted passing through the center of the cube, one for each axis. These sections are then stacked in the form of an RGB image, with each section assuming the values of one of the color channels. This process is illustrated in Figure 1.

In the case of data used for training and network validation, each example must be associated with a label that identifies the expected output. Two approaches were used to generate the seismic data and the facies labels for the patch-based training set: using well logs and seismic from a region around the well; and from patches manually classified in specified regions of the seismic cube.

A. Network Architecture

The network topology developed for this work is composed of four blocks: the first three are a sequence of a convolutional layer (which are always followed by ReLU activation), then a pooling layer and a dropout layer; the last block is a fully connected layer before a softmax activation. An overview of this architecture is illustrated in Figure 2, the abbreviations **c**, **p**, **fc** and **s** stand for convolution layer, max-pooling layer, fully

connected layer and stride, respectively. The number following **c** and **p** indicates the size of a square window used for the operation, while the number of filters or units are marked at the end of the convolution and fully connected layers.

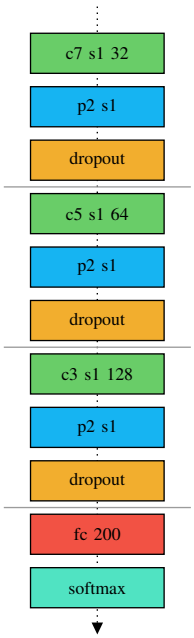

Fig. 2: Diagram of the network architecture used in this work. The letters **c**, **p** and **fc** are used to abbreviate convolution, max pooling and fully connected layers.

The Python programming language was used to implement the method. The libraries used were: Keras, for definition, training, and testing of convolutional network models; Tensorflow as *backend* from the Keras library; Matplotlib and K3D for viewing data and results. The code produced during this work can be found in the GitHub repository at: *https://github.com/thurbridi/cnn-facies-classifier*

Since this sampling method generates a great deal of redundant data compared to the original seismic cube, it was necessary to implement training and prediction methods using Keras Sequence object, which streamlines multiprocessing and loads only the necessary examples for each epoch to memory.

IV. Experimental Results

As mentioned in section II, seismic data is obtained through indirect measurements of the subsurface and it's interpretation to seismic facies is not trivial. This data is usually made available as 3D volumes of reflection values processed from seismic acquisition.

In the problems relating to seismic data segmentation, ground truth data often comes from a specialist that interprets a limited number of examples. In the case of data used for supervised machine learning training and validation, each example must be associated with a label that identifies the expected output. However, different researchers may annotate different classes, or use different train and test splits [11].

Two approaches can be used to generate the seismic data and the facies labels that will make up the training set:

- The training set can come from well information - which can be viewed as a line, approximately vertical, that crosses the seismic cube. For each of the facies values classified in the well, we sample the region around the value from the seismic cube, that is, we slide a cube centered along the line of the well that crosses the seismic data, performing the sampling process described above and associating the values of classified facies;
- The training set can also be formed by data from classifications made manually by specialists in patches or small tiles in specified regions of the seismic cube.

Two distinct test scenarios were employed in this study: the Stanford VI-E synthetic reservoir, which was originally created by Castro et al. (2005), and represents a three-layer prograding fluvial channel system; and block F3, a real seismic survey acquired in the North Sea, offshore Netherlands, which is freely accessible by the geoscience research community.

In the first scenario, the training set was built using data from some wells randomly spread across the cube. In the second scenario, the patch based training data was obtained from the public database made available by Alaudah et al. [11]. We scrutinize their results in order to compare our proposal with other research that classifies seismic facies using CNNs in a purely two-dimensional approach.

A. Seismic Facies Segmentation in the Stanford VI-E

The Stanford VI-E reservoir [23] is a synthetic reservoir model created with the aim of testing modeling, characterization, and reservoir production algorithms. It is an extensive data set with more than 6 million cells containing petrophysical properties and seismic attributes. The data are available in a volume of size $150 \times 200 \times 200$ cells. The cells have dimensions 25m in the horizontal axes x and y and 1m in the vertical axis z. Therefore, the reservoir has an extension of 3,750m in the east-west direction, 5,000m in the north-south direction and 200m in depth.

The stratigraphic model of the reservoir fluvial channel system prograding into the basin located toward the north of the reservoir. deltaic deposits (layer 3) were formed first and meandering channels (layer 2) and then sinuous channels (layer 1) were deposited in this fluvial channel system. Layers 1 and 2 are composed of four facies: *floodplain* (clay deposits), *pointbar* (sand deposits that occur along the inner convex edges), *channel* (sand deposits), and textitboundary (clay edge). The deltaic Layer contains only the *floodplain* and *channel* facies [23].

Figure 4 illustrates the complete reservoir (upper left corner) and layers 1, 2 and 3 (upper right, lower left and lower right, respectively).

Seismic facies were mapped to classes of the classification problem by assigning a numerical code to each one:

- *floodplain*: class 0;
- *pointbar*: class 1;

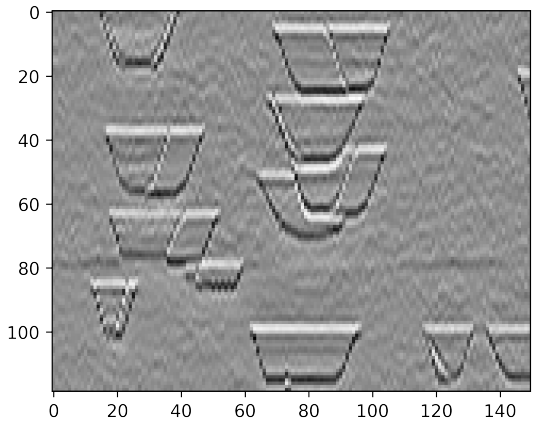

(a) inline 30

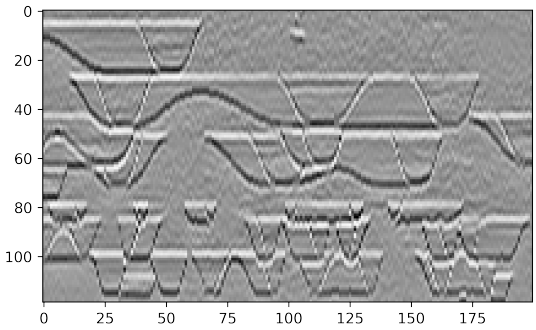

(b) crossline 80

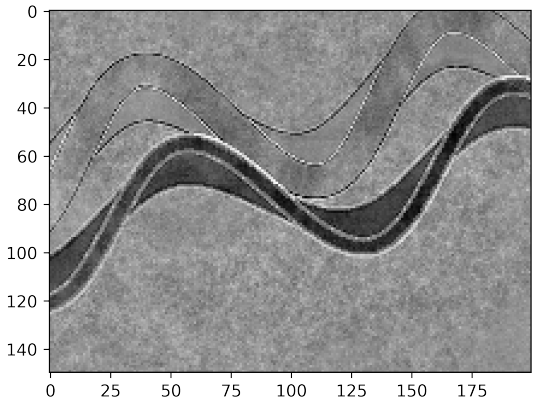

(c) depth 70

Fig. 3: Orthogonal Planes seismic sections from the Stanford VI-E reservoir cube.

- *channel*: class 2;
- *boundary*: class 3.

In our experiment we train and use the TOP-CNN to segment the classes in layers 1 and 2. Basically the idea is to test the method's capability to classify classes 2 (*pointbar*), 3 (*channel*) and 4 (*boundary*) when trained with different levels of sinuosity.

In order to set up our training set using the seismic traces and classified facies around oil wells approach, we randomly create 10 pseudo-wells in Stanford VI-E cube (originally this

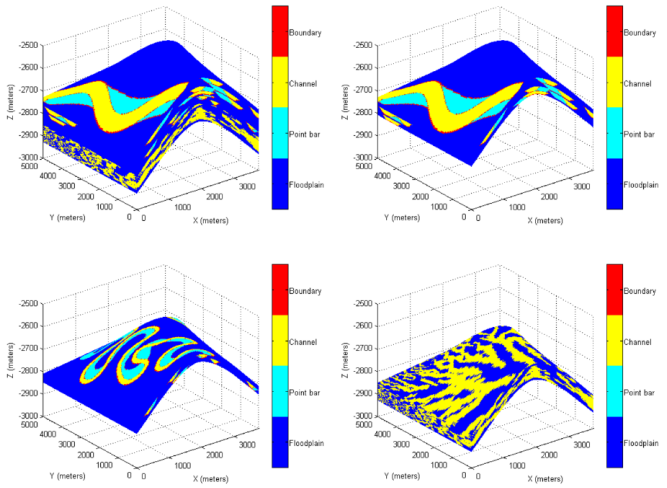

Fig. 4: Stratigraphic model of the Stanford VI-E reservoir [23].

synthetic model does not have defined wells). So, 10 random x and y positions of the seismic cube were chosen, each representing the position of a pseudo-well. Moving along the z axis in these positions, cubes of size $32 \times 32 \times 32$ are sampled. The label for each of these samples is extracted from the ground truth reservoir's facies volume in the position corresponding to the center of the sample.

When analyzing the training data set (Figure 5), we observed that class 0 (*floodplain*) is much more frequent than other classes, which is expected based on the reservoir structures (Figure 4). However, the learning of unbalanced classes is a known problem in the area of *machine learning*. [24] presents a review on state of the art solutions for this problem. In our experiment, we made class balance using the *Random Oversampling* algorithm that randomly repeats examples from the less frequent classes. After balancing, the brightness values for each orthogonal plane image were normalized to the $[0, 1]$ interval and 20% of the data was reserved for the validation set. The resulting class distribution can be seen in Figure 6.

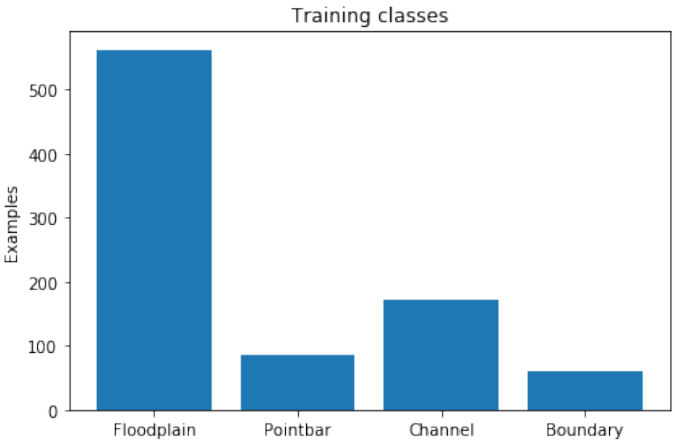

Fig. 5: Class frequency of training examples.

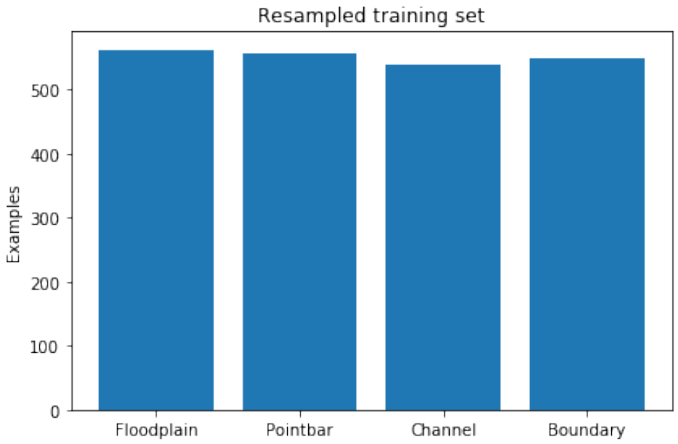

Fig. 6: Class frequency of training examples after random oversampling.

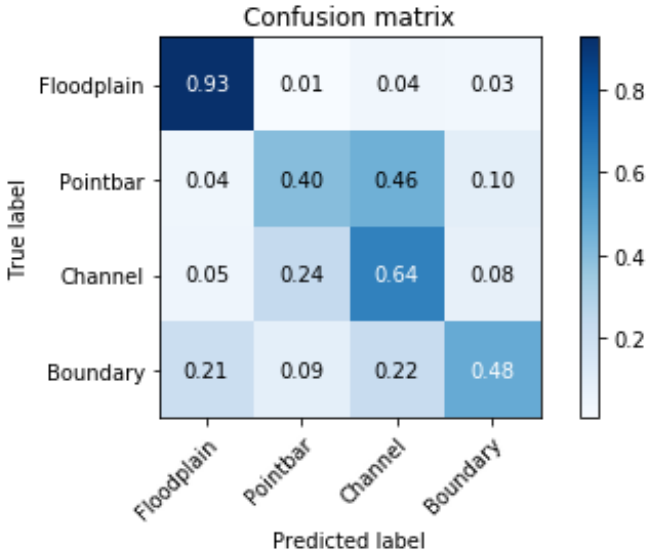

Fig. 7: Confusion matrix from the Stanford VI-E dataset.

After trained with with pseudo-wells data, the model was applied across the whole seismic cube and performance metrics was calculated. The model showed an average accuracy of 0.89 which means a high rate of true positives and true negatives between classes. $Precision_M$ value indicates that, on average, 60% of the points classified as a given facies were correctly predicted and the $recall_M$ value indicates that, on average, 61% of the points of a facies are classified correctly.

Analyzing the confusion matrix, shown in Figure 7, we can observe that, while class 0 had 93% of correct predictions, our model had some difficulties in correctly classify between classes 2 and 3. As pointed out by [23], both classes are composed of sandstones with very similar impedance values (see Figure 3), so that their seismic amplitude responses are very similar. Since the *boundary* (class 3) is a very thin structure between the *floodplain* (class 0) and *channel* (class 2) structures, we can notice that many times the model incorrectly classify the right class.

Figure 8 shows the classes ground truth (above) compared with result of the network forecast in the first two layers of the Stanford VI-E reservoir. In this figure, class 0 (*floodplain*) is made transparent to highlight the reservoir's river structures. Classes 1, 2 and 3 are represented by the colors blue, green and yellow in that order. With this 3D visualization, it is interesting to note that class 3, despite the low precision in the confusion matrix, still has part of its structure recovered given its occurrence in thin layers only at the edges between classes. Visually, the net result also seems to get worse in the second layer of the reservoir, where the channels become shallower, narrower and more sinuous.

B. Seismic Facies Segmentation in the F3 Block

Located next to Netherlands coast, the F3 block covers an area of 16km $\times$ 24km and was mapped with 3D seismic surveys for oil and gas exploration. As mentioned in Section II and at the beginning of this section, Alaudah et al. [11] processed part of this block to create a benchmark, annotating the entire volume and dividing it into 3 sets, one for training and two sets for final testing. The benchmark features 6 different classes (seismic facies) separated by their seismic response and formation period, listed below:

0) **Upper North Sea**: claystones and sandstones from Miocene to Quaternary;
1) **Middle North Sea**: sands, sandstones, and claystones from Paleocene to Miocene;
2) **Lower North Sea**: same composition of Middle North;
3) **Chalk/Rijnland**: carbonates of Upper Cretaceous and Paleocene; clay formations with sandstones of Upper Cretaceous;
4) **Scruff**: claystones of Upper Jurassic and Lower Cretaceous;
5) **Zechstein**: evaporites and carbonates of Zechstein.

These classes can be visualized in Figure 9: Upper North in red, Middle North in green, Lower North in yellow, Chalk/Rijnland in blue, Scruff in orange and Zechstein in purple.

As reported in Section II, in addition to the annotated dataset, [11] presents two alternatives (patch-based and section-based) to serve as baseline models to train and test their encoder-decoder network topology. Using their annotated dataset, we trained our model with different patch sizes (32×32, 48×48, 64×64), making use of the whole training cube with a $80/20$ training/validation split.

After validation loss converged, we ran our models on the test data and calculated the same metrics used for the benchmark's models, which are:

- Pixel Accuracy (PA), is the percentage of pixels over all classes that are correctly classified;
- Class Accuracy (CA), is the percentage of pixels that are correctly classified in a class i.

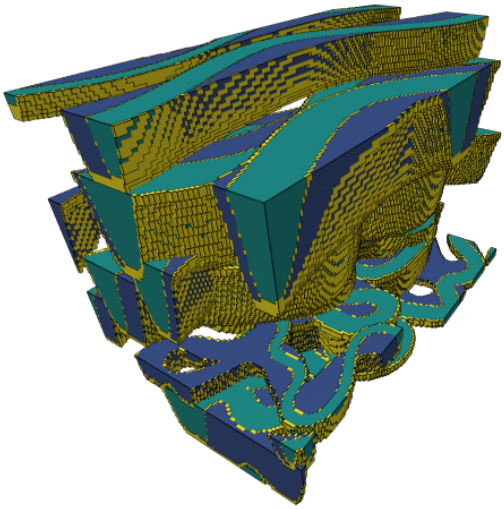

(a) Stanford VI-E ground truth 3D model.

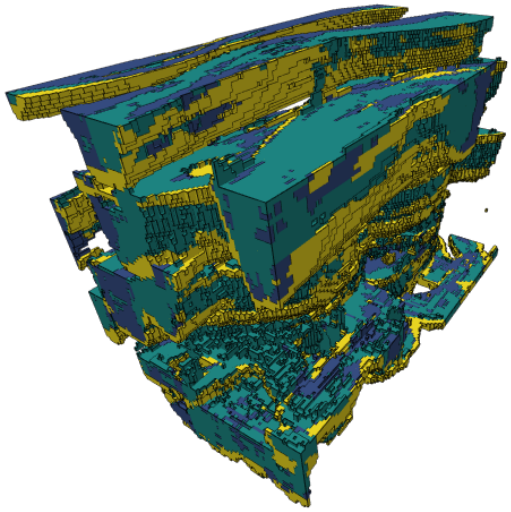

(b) TOP-CNN reconstruction of the Stanford VI-E reservoir.

Fig. 8: Comparison between the original model (a) and our trained network prediction (b) on the Stanford VI-E reservoir. Green corresponds to *channel*, Blue corresponds to *pointbar* and Yellow corresponds to *boundary*.

- Mean Class Accuracy (MCA), is the average of CA over all classes; and
- Frequency-Weighted Intersection over Union (FWIU), is the measure of the overlap between the set of pixels that belong to class i and the set of pixels classified as class i averaged over all classes and each class is weighted by its size.

Table I lists our results as well as Alaudah's results for their patch-based dataset. In bold is the best result for each metric.

With the results presented in Table I, we note that bigger sampling windows (thus bigger input image size) favored more massive classes, especially Lower N., where we achieve 0.98

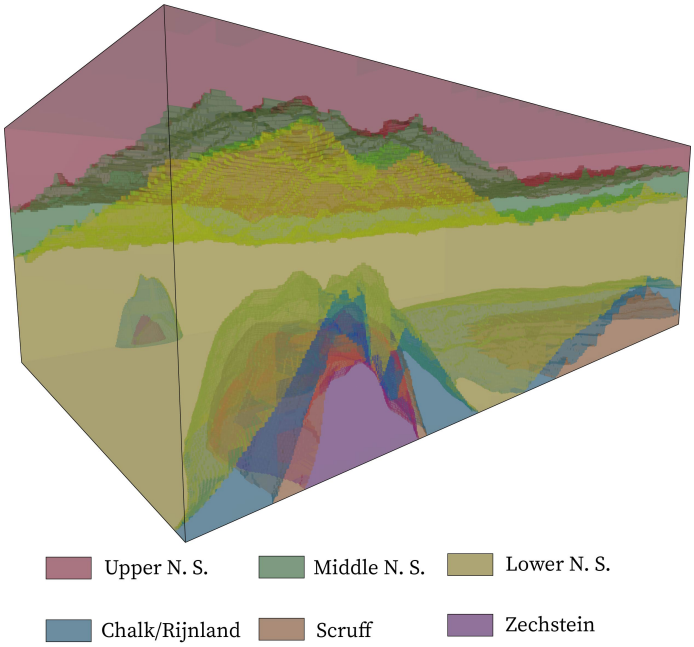

Fig. 9: 3D view of the geological facies in the training partition of the F3 block.

class accuracy. TOP-CNN 64×64 patch size model presents a better performance when using the Pixel Accuracy and the Frequency-Weighted Intersection over Union metrics, while the 32×32 patch size model has a better Class Accuracy in three over six class classification and achieve the best Mean Class Accuracy over all other models.

In comparison to Alaudah's Patch-based model, our TOP-CNN approach surpassed most metrics (except Lower N. Class Accuracy) when not using data augmentation for training. However, we took class imbalance into account by using Keras class weights for weighting the loss function during training. It is important to note that despite using 2D convolutional networks in the traditional way, Alaudah et al. apply their model in inlines and crosslines and makes an average where the same points are evaluated [11].

V. Conclusion

In this work, we have introduced the Three Orthogonal Planes Convolutional Neural Network model to efficiently perform the semantic segmentation and facies classification of 3D seismic cubes. The main idea of this model is to be able to capture some spatial correlations between 3D image voxels making it a computationally less complex alternative than using 3D convolutional networks.

Our proposed model were evaluated on a synthetic data of the Stanford VI-E reservoir and on real data in a benchmark based on the F3 block. Two approaches were used to generate the seismic data and the facies labels for the patch-based training set: using well logs and seismic from a region around the well; and from patches manually classified in specified regions of the seismic cube. The results show a strong semantic

TABLE I

Metric / Model	PA	Class Accuracy						MCA	FWIU
		Zechstein	Scruff	Rijnland/Chalk	Lower N. S.	Middle N. S.	Upper N. S.		
TOP-CNN w 32×32 patch size	0.86	**0.71**	**0.31**	0.59	0.93	0.90	**0.96**	**0.73**	0.76
TOP-CNN w 48×48 patch size	0.87	0.59	0.24	0.63	0.96	0.89	0.95	0.71	0.78
TOP-CNN w 64×64 patch size	**0.88**	0.26	0.22	0.60	0.98	0.86	0.95	0.64	**0.79**
Patch-based model	0.788	0.264	0.074	0.499	**0.992**	0.804	0.754	0.565	0.640
Patch-based + aug.	0.852	0.434	0.221	**0.707**	0.974	0.884	0.916	0.689	0.743
Patch-based + aug + skip	0.862	0.458	0.286	0.673	0.974	**0.912**	0.926	0.705	0.757

modeling capability surpassing, in most cases, the results presented by another 2D CNN model on the same data.

As future work we consider working on data augmentation techniques and the use of transfer learning instead of training our models from scratch. Another point that deserves attention is to expand the model to an encoder-decoder architecture in order to verify an increase in performance as reported for 2D CNNs in other researches and the addition of other non-orthogonal planes in order to try to capture other voxels correlations. In addition, currently forecasting is done pixel by pixel. In the future we intend to evaluate the forecast made in a pixel neighborhood in order to be able to further increase the accuracy.

REFERENCES

[1] J. R. Fanchi, "Chapter 10 - fundamentals of reservoir characterization," in *Shared Earth Modeling*, J. R. Fanchi, Ed. Woburn: Butterworth-Heinemann, 2002, pp. 170 – 181. [Online]. Available: http://www.sciencedirect.com/science/article/pii/B9780750675225001000

[2] M. M. Roksandić, "Seismic facies analysis concepts *," *Geophysical Prospecting*, vol. 26, no. 2, pp. 383–398, 1978. [Online]. Available: https://www.earthdoc.org/content/journals/10.1111/j.1365-2478.1978.tb01600.x

[3] W. Li, "Classifying geological structure elements from seismic images using deep learning," in *SEG Technical Program Expanded Abstracts 2018*, 2018, pp. 4643–4648. [Online]. Available: https://library.seg.org/doi/abs/10.1190/segam2018-2998036.1

[4] T. Zhao, "Seismic facies classification using different deep convolutional neural networks," in *SEG Technical Program Expanded Abstracts 2018*, 09 2018, pp. 2046–2050. [Online]. Available: https://library.seg.org/doi/abs/10.1190/segam2018-2997085.1

[5] D. S. Chevitarese, D. Szwarcman, E. V. Brazil, and B. Zadrozny, "Efficient classification of seismic textures," in *2018 International Joint Conference on Neural Networks (IJCNN)*, July 2018, pp. 1–8.

[6] M. Jervis, M. Liu, and P. Nivlet, "Deep learning applied to seismic facies classification," in *2019 New Advances in Seismic Interpretation Workshop*, 03 2019.

[7] M. Liu, W. Li, M. Jervis, and P. Nivlet, "3d seismic facies classification using convolutional neural network and semi-supervised generative adversarial network," in *SEG Technical Program, Expanded Abstracts 2019 (Society of Exploration Geophysicists, Tulsa, OK, 2019)*, 08 2019, pp. 4995–4999.

[8] G. Zhao and M. Pietikainen, "Dynamic texture recognition using local binary patterns with an application to facial expressions," *IEEE Transactions on Pattern Analysis and Machine Intelligence*, vol. 29, no. 6, pp. 915–928, June 2007.

[9] V. Andrearczyk and P. F. Whelan, "Convolutional neural network on three orthogonal planes for dynamic texture classification," *Pattern Recognition*, vol. 76, pp. 36 – 49, 2018. [Online]. Available: http://www.sciencedirect.com/science/article/pii/S0031320317304375

[10] A. Pourtaherian, F. Ghazvinian Zanjani, S. Zinger, N. Mihajlovic, G. Ng, H. Korsten, and P. With, "Robust and semantic needle detection in 3d ultrasound using orthogonal-plane convolutional neural networks," *International Journal of Computer Assisted Radiology and Surgery*, vol. 13, 05 2018.

[11] A. Yazeed, M. Patrycja, A. Motaz, and A. Ghassan, "A machine learning benchmark for facies classification," *Interpretation*, vol. 7, pp. 1–51, 05 2019.

[12] C. L. Liner and T. A. McGilvery, *The Art and Science of Seismic Interpretation*. Springer, 2019, https://www.springer.com/gp/book/9783030039967.

[13] J. Mitchum, R. M., P. R. Vail, and J. B. Sangree, "Seismic Stratigraphy and Global Changes of Sea Level, Part 6: Stratigraphic Interpretation of Seismic Reflection Patterns in Depositional Sequences1," in *Seismic Stratigraphy — Applications to Hydrocarbon Exploration*. American Association of Petroleum Geologists, 01 1977. [Online]. Available: https://doi.org/10.1306/M26490C8

[14] T. ColÉou, M. Poupon, and K. Azbel, "Unsupervised seismic facies classification : A review and comparison of techniques and implementation," *The Leading Edge*, vol. 22, no. 10, p. 942, 2003. [Online]. Available: http://dx.doi.org/10.1190/1.1623635

[15] T. Zhao, V. Jayaram, A. Roy, and K. J. Marfurt, "A comparison of classification techniques for seismic facies recognition," *Interpretation*, vol. 3, no. 4, pp. SAE29–SAE58, 2015. [Online]. Available: https://doi.org/10.1190/INT-2015-0044.1

[16] J. S. Dramsch and M. Lüthje, *Deep-learning seismic facies on state-of-the-art CNN architectures*. SEG - Society of Exploration Geophysicists, 2018, pp. 2036–2040. [Online]. Available: https://library.seg.org/doi/abs/10.1190/segam2018-2996783.1

[17] W. Burton, "2d or 3d? a simple comparison of convolutional neural networks for automatic segmentation of cardiac imaging," https://towardsdatascience.com/2d-or-3d-a-simple-comparison-of-convolutional-neural-networks-for-automatic-segmentation-of-625308f52aa7, Apr. 2019.

[18] Y. Jiang, "Detecting geological structures in seismic volumes using deep convolutional neural networks," Master's thesis, Rheinisch-Westfälische Technische Hochschule Aache, 2017.

[19] X. Wu, L. Liang, Y. Shi, and S. Fomel, "Faultseg3d: Using synthetic data sets to train an end-to-end convolutional neural network for 3d seismic fault segmentation," *GEOPHYSICS*, vol. 84, no. 3, pp. IM35–IM45, 2019. [Online]. Available: https://doi.org/10.1190/geo2018-0646.1

[20] H. R. Roth, H. Oda, X. Zhou, N. Shimizu, Y. Yang, Y. Hayashi, M. Oda, M. Fujiwara, K. Misawa, and K. Mori, "An application of cascaded 3d fully convolutional networks for medical image segmentation," *Computerized Medical Imaging and Graphics*, vol. 66, pp. 90 – 99, 2018. [Online]. Available: http://www.sciencedirect.com/science/article/pii/S0895611118301472

[21] J. Dolz, C. Desrosiers, and I. B. Ayed, "3d fully convolutional networks for subcortical segmentation in mri: A large-scale study," *NeuroImage*, vol. 170, pp. 456 – 470, 2018, segmenting the Brain. [Online]. Available: http://www.sciencedirect.com/science/article/pii/S1053811917303324

[22] K. Kamnitsas, C. Ledig, V. F. Newcombe, J. P. Simpson, A. D. Kane, D. K. Menon, D. Rueckert, and B. Glocker, "Efficient multi-scale 3d cnn with fully connected crf for accurate brain lesion segmentation," *Medical Image Analysis*, vol. 36, pp. 61 – 78, 2017. [Online]. Available: http://www.sciencedirect.com/science/article/pii/S1361841516301839

[23] J. Lee and T. Mukerji, "The stanford vie reservoir : A synthetic data set for joint seismic-em time-lapse monitoring algorithms," 25th Annual Report, Stanford Center for Reservoir Forecasting, Stanford University, Stanford, CA., Tech. Rep., 2012.

[24] H. He and E. A. Garcia, "Learning from imbalanced data," *IEEE Transactions on Knowledge and Data Engineering*, vol. 21, no. 9, pp. 1263–1284, Sep. 2009.